

Dielectric, ferroelectric, and piezoelectric behaviors of $\text{AgNbO}_3\text{-KNbO}_3$ solid solution

Desheng Fu,^{1,2,a)} Mitsuru Itoh,³ and Shin-ya Koshihara^{2,4}

¹Division of Global Research Leaders, Shizuoka University, Johoku 3-5-1, Naka-ku, Hamamatsu 432-8561, Japan

²Exploratory Research for Advanced Technology (ERATO), Japan Science and Technology Agency (JST), 3-5 Sanbanchou, Chiyoda-ku, Tokyo 102-0075, Japan

³Materials and Structures Laboratory, Tokyo Institute of Technology, 4259 Nagatsuta, Yokohama 226-8503, Japan

⁴Frontier Collaborative Research Center and Department of Materials Science, Tokyo Institute of Technology, Meguro-ku, Tokyo 152-8551, Japan

(Received 13 July 2009; accepted 10 October 2009; published online 17 November 2009)

Phase evolution in the $(\text{Ag}_{1-x}\text{K}_x)\text{NbO}_3$ (AKN) solid solution was investigated by x-ray diffraction, dielectric, and ferroelectric measurements. At room temperature, there are three phase boundaries at $x_{c1} \approx 0.07$, $x_{c2} \approx 0.20$, and $x_{c3} \approx 0.8$. When $x_{c1} < x$, AKN transforms from the AgNbO_3 -type orthorhombic phase with a weak ferroelectricity into a new orthorhombic phase with a strong ferroelectricity. This ferroelectric phase is stable for $x_{c1} < x < x_{c2}$, and shows a nearly composition-independent Curie point of 525 K and a very large polarization ($P_r = 20.5 \mu\text{C}/\text{cm}^2$ for a ceramics sample of $x = 0.1$). When $x_{c2} < x < x_{c3}$, single-phase AKN was not available. When $x_{c3} < x$, AKN adopts the KNbO_3 -type orthorhombic structure and shows similar successive phase transitions to pure KNbO_3 . Its Curie point increases linearly with x from 633 K for $x = 0.80$ to 696 K for $x = 1.00$. We obtained a strain level of $\approx 0.05\%$ and a d_{33} value of 46–64 pC/N for the AKN ceramics samples. The relationship between the structural change and ferroelectric phase evolution is also discussed briefly. © 2009 American Institute of Physics. [doi:10.1063/1.3259410]

I. INTRODUCTION

In the course of seeking lead-free piezoelectric materials,^{1–7} we found a very large polarization ($\approx 52 \mu\text{C}/\text{cm}^2$) in AgNbO_3 polycrystals under the application of an electric field of 220 kV/cm.³ Such large polarization is suggested to be due to the large local displacement of Ag ions in the perovskite structure.^{4,8,9} Despite the exact structure of AgNbO_3 is still unresolved, both first-principles calculations^{8,9} and structural analysis¹⁰ indicate that Ag ions are ordering in an antiferroelectric (AFE) manner at room temperature in AgNbO_3 . Experimentally, at a weak electric field, only an extremely small remanent polarization ($P_r \sim 0.041 \mu\text{C}/\text{cm}^2$)^{11,12} was observed in AgNbO_3 , which was believed to be derived from the very small displacement of Nb ions in the structure.^{3,8} In order to induce a strong ferroelectric (FE) state in AgNbO_3 , in addition to the application of a strong electric field, the chemical modification may be useful. In fact, very large spontaneous polarization was realized in $\text{Ag}_{1-x}\text{Li}_x\text{NbO}_3$ solid solution ($P_s = 40 \mu\text{C}/\text{cm}^2$ for 6.2 mol % Li)^{4,13} by using substitution of Li that generally has a strong off-centering nature in the perovskite structure.^{13,14}

Because of a low tolerance factor ($t < 1$) due to the small ionic radius of Ag^+ (1.28 Å),¹⁵ AgNbO_3 adopts a deformed perovskite structure with a large tilting of oxygen octahedrons along the three axes of a pseudocubic structure at room temperature (see Fig. 1).¹⁰ Such octahedral tilting facilitates the AFE ordering, but hinders the FE ordering.^{8,9} Similar to

the case of alloying AFE- PbZrO_3 with FE- PbTiO_3 to form a solid solution with good piezoelectric and FE performances,¹⁶ alloying AgNbO_3 with other FE materials may also lead to the discovery of new materials with good piezoelectric and FE properties. Among the FE niobate perovskites, KNbO_3 has a high Curie point ($T_c = 696$ K) and a large P_s ($= 41 \mu\text{C}/\text{cm}^2$ at room temperature);^{17,18} therefore, it is promising to form a $\text{AgNbO}_3\text{-KNbO}_3$ solid solution

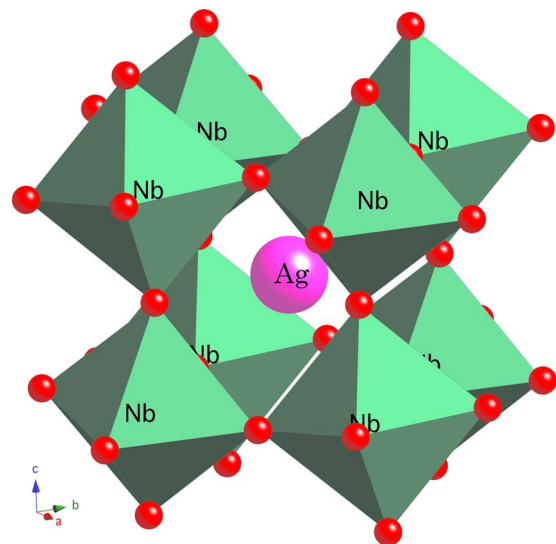


FIG. 1. (Color online) Schematic structure of the AgNbO_3 perovskite at room temperature (Ref. 10). Oxygen octahedrons tilt strongly along the three axes of the cubic structure because of the low tolerance factor due to the small ionic radius of Ag^+ .

^{a)}Electronic mail: ddsfu@ipc.shizuoka.ac.jp.

with interesting physical properties. Despite the possibility of good ferroelectricity in this system, the reports on $\text{AgNbO}_3\text{--KNbO}_3$ solid solution are very limited.^{19–21} Early report suggested that there may be an occurrence of a critical point in $\text{Ag}_{1-x}\text{K}_x\text{NbO}_3$ (AKN) at $x=0.05\text{--}0.06$ on the basis of the dielectric measurements.¹⁹ However, it was also reported that K substitution has no effect on the dielectric behaviors of AKN for $x\leq 0.04$.²¹ On the other hand, for a K-rich region, it was reported that merely 6 mol % Ag can enter the K site of the KNbO_3 structure.²⁰ Apparently, there is a lack of systematical understanding of the phase evolution and the physical properties of this system, which is therefore the focus of the present study. In Secs. II and III, we will show the synthesis, and the structural, dielectric, FE, and piezoelectric properties of the AKN solid solutions. We will also make a brief discussion on the ferroelectricity and structure change in this system.

II. EXPERIMENTAL

The AKN polycrystals were prepared by a solid state reaction method. Appropriate amounts of high purity Ag_2O , Nb_2O_5 , and K_2CO_3 were mixed homogeneously with ethanol. Calcination was then performed at 1173 K for 6 h in O_2 atmosphere with a slow heating rate of 1 K/min. The calcined powder was milled again, pressed in a 6 mm steel die with a pressure of 10 MPa to form the pellets, which were then preheated at 773 K for 2 h, followed by a sintering at temperature of 1253–1323 K (1323 K for $x=0\text{--}0.1$ and 1.00, 1273 K for $x=0.15$ and 0.90, and 1253 K for $x=0.17$ and 0.80, respectively) for 3 h in O_2 atmosphere. The atmosphere and heating rate are found to have great influences on the phase stability of the AKN solid solution.

X-ray diffraction technique was used to determine the structure and lattice parameters of the AKN solid solution. To measure the electrical properties, the sintered pellet was polished and fired with Au paint at 823 K in O_2 for 1 h. Dielectric measurements were performed at a weak field of 1 V/mm using a Hewlett-Packard Precision LCR meter (HP4284A) in the temperature range 2.5–850 K. $D\text{--}E$ and strain electric-field ($S\text{--}E$) hysteresis loops were measured at room temperature with a FE measurement system of an aix-ACCT TF Analyzer 2000 equipped with a Canon DS-80 interferometer and a high voltage source. Piezoelectric coefficients d_{33} were evaluated at room temperature by a piezo- d_{33} meter (Institute of Acoustics, Chinese Academy of Science, ZJ-3B). The samples poled by an electric field of 20 kV/cm at $T\approx 410$ K for about 30 min were used for d_{33} and unipolar-field strain measurements.

III. RESULTS AND DISCUSSIONS

A. X-ray diffraction patterns

Figure 2 shows the x-ray diffraction patterns of the obtained samples, from which we can clearly see the phase evolution with composition at room temperature in the $\text{AgNbO}_3\text{--KNbO}_3$ system. There are four regions separated by three phase boundaries located at $x_{c1}\approx 0.07$, $x_{c2}\approx 0.20$, and $x_{c3}\approx 0.80$, respectively. When $x < x_{c1}$, AKN solid solution maintains the orthorhombic phase of pure AgNbO_3 .

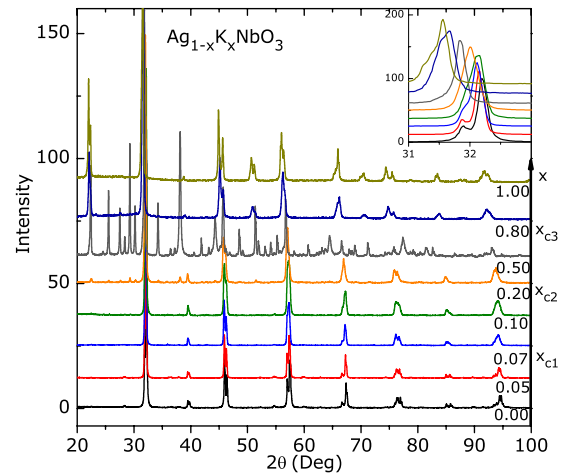


FIG. 2. (Color online) Powder x-ray diffraction patterns of $\text{Ag}_{1-x}\text{K}_x\text{NbO}_3$ solid solutions at room temperature. The inset shows the variation of the main diffraction peak from the (110) plane of the pseudocubic structure. There are three phase boundaries for the phase evolution at $x_{c1}\approx 0.07$, $x_{c2}\approx 0.20$, and $x_{c3}\approx 0.80$, respectively. For $x_{c2} < x < x_{c3}$, single-phase AKN was not obtained.

When $x > x_{c1}$, however, a different orthorhombic phase is formed and stable in the composition range of $x_{c1} < x < x_{c2}$.

For a wide composition range of $x_{c2} < x < x_{c3}$, it is difficult to prepare single-phase AKN by the present process. As shown in the diffraction patterns of $x=0.50$ in Fig. 2, in addition to the AKN phase, $\text{K}_{5.75}\text{Nb}_{10.85}\text{O}_{30}$ -type phase and metal silver phase were always observed in the compounds. It seems that the formation of a $\text{K}_{5.75}\text{Nb}_{10.85}\text{O}_{30}$ -type phase is very likely due to the easy precipitation of metal silver for this composition range. The inset of Fig. 2 shows a gradual shift of the main diffraction peak from the (110) plane of a pseudocubic structure to a lower angle with the increase in x . This suggests that a pure AKN solid solution may be available for these compositions by a proper process, such as high pressure synthesis. Apparently, the difficulties in getting a single phase for these compositions are related to the large difference of ionic radius between Ag^+ (1.28 Å) and K^+ (1.69 Å),¹⁵ and to the easy decomposition of silver oxide into metal silver at high temperature.

In the K-rich region $x > x_{c3}$, AKN has the FE orthorhombic structure of pure KNbO_3 . It is known that KNbO_3 ceramics, which are slightly of stoichiometry, swell and disintegrate in air within a short time.¹⁶ However, such phenomenon has not been observed in the AKN solid solution. In comparison with the low solid-solution limit (about 6 mol % of Ag in the K site) reported by Weirauch,²⁰ we found that this limit was expanded greatly by the present process (about 20 mol % of Ag in the K site). Apparently, this solid-solution limit is dependent on the process. We used a low heating rate (1 K/min) and an oxygen atmosphere, which facilitate to stabilize the phase of the AKN solid solution; in contrast, Weirauch *et al.*²⁰ synthesized their samples in an air atmosphere.

B. Dielectric behaviors

In order to understand the phase evolution with temperature, we examined the dielectric behaviors in a wide tem-

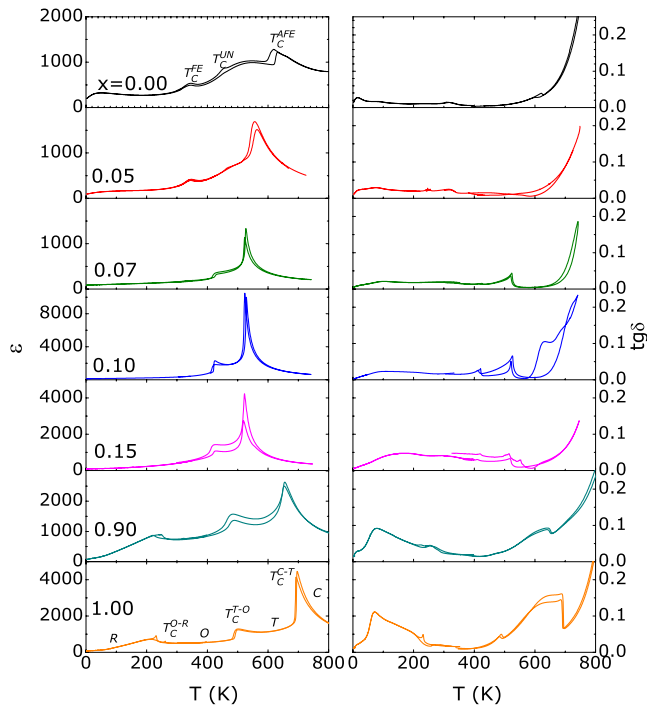


FIG. 3. (Color online) Temperature dependence of dielectric constant and loss.

perature range 2.5–850 K. The results are given in Fig. 3. For pure AgNbO_3 , there are detectable dielectric anomalies at temperatures of $T_c^{\text{FE}} \approx 340$ K, $T_c^{\text{UN}} \approx 454$ K, and $T_c^{\text{AFE}} \approx 624$ K, respectively.³ Despite these observed dielectric anomalies, a recent structural analysis using synchronistic x-ray and neutron diffractions does not detect any change in the space group in the temperature range of $T < T_c^{\text{AFE}}$.¹⁰ Phase transition at T_c^{FE} is considered to be driven by a weak FE ordering on the basis of remanent polarization measurements.¹² The nature of dielectric anomaly at T_c^{UN} is still unclear.³ AFE phase transition was proposed to occur at T_c^{AFE} on the basis of the pressure dependence of this transition temperature.²² As shown in Fig. 3, AKN with $x < x_{c1}$ has a great similarity of dielectric behaviors to pure AgNbO_3 . This indicates that AKN with $x < x_{c1}$ has the same phase evolution of pure AgNbO_3 . The observed difference between them is that there is a large decrease in T_c^{AFE} and a large change in dielectric constant for this transition with the increase in x .

When $x \geq x_{c1} = 0.07$, AKN shows a completely different temperature dependence of dielectric constant. The very sharp peak of dielectric constant is similar to that of paraelectric (PE) phase transition in the normal FE materials such as KNbO_3 , indicating that the AFE state has changed into a normal FE state for $x > x_{c1}$. This result is in good agreement with the observations of x-ray diffractions and with the early report of Łukaszewski¹⁹ who suggested a structural transformation at $x = 0.05$ – 0.06 . Within the composition range of $x_{c1} < x < x_{c2}$, the dielectric behaviors exhibit several notable features: (1) The magnitude of dielectric constant at the Curie point is greatly larger than the maximum of AgNbO_3 and a high value of $\sim 10^4$ was observed for a ceramics sample of $x = 0.10$. (2) In addition to the Curie point at

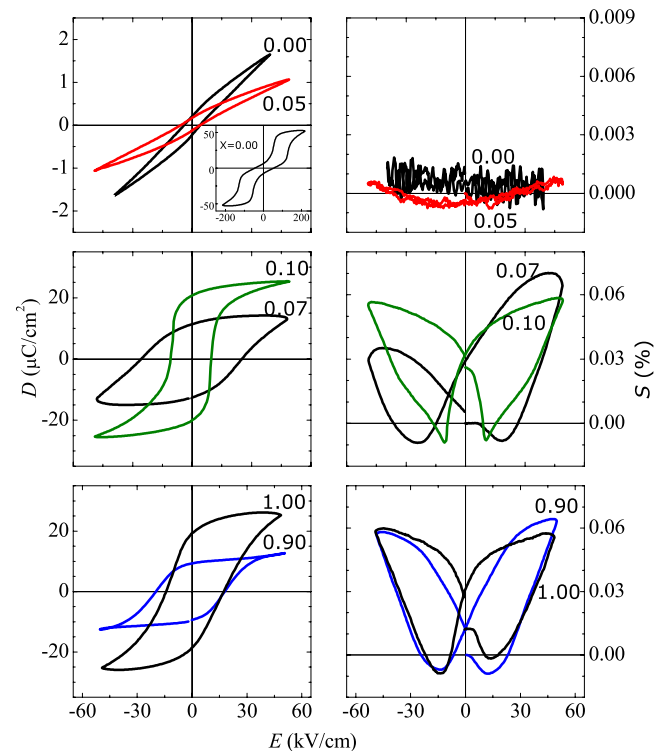


FIG. 4. (Color online) D - E and S - E hysteresis loops obtained with the ceramics samples at room temperature. The inset shows the AFE loop of pure AgNbO_3 (Ref. 3).

$T \sim 525$ K, there is another FE phase transition at $T \sim 420$ K, below which no dielectric anomaly was detected down to the lowest temperature (2 K) of our measurement system. This indicates that the FE orthorhombic phase in AKN with $x_{c1} < x < x_{c2}$ is extremely stable. Such case is rare in FE perovskite oxides of titanate or niobate. (3) More surprisingly, these two transition temperatures are nearly insensitive to the concentration of K substitution, supporting the early result of Łukaszewski.¹⁹ These anomalous characteristics indicate that AKN with $x_{c1} < x < x_{c2}$ may have an interesting mechanism of FE ordering.

When $x > x_{c3}$, AKN shows dielectric behaviors similar to that of pure KNbO_3 . There are three successive phase transitions corresponding to cubic-tetragonal (C - T), tetragonal-orthorhombic (T - O), and orthorhombic-rhombohedral (O - R) transitions at T_c^{C-T} , T_c^{T-O} , and T_c^{O-R} , respectively.¹⁷ All these transition temperatures increase gradually with the increase in x . In addition, all these phase transitions have a thermal hysteresis, and are first order in nature.

C. Ferroelectricity and piezoelectricity

The dielectric behaviors of AKN with $x_{c1} < x < x_{c2}$ and $x > x_{c3}$ indicate that a FE state with a large P_s should have been established in these solid solutions at room temperature. Since there is no report on the FE and piezoelectric behaviors for the AKN solid solutions, we thus performed D - E and S - E loop measurements to examine their ferroelectricity and piezoelectricity. Some typical results are given in Fig. 4. Similar to pure AgNbO_3 ,³ merely a small P_r was observed in AKN samples with $x < x_{c1}$. In sharp contrast, when $x > x_{c1}$, a normal square D - E loop was observed. A large value of P_r ,

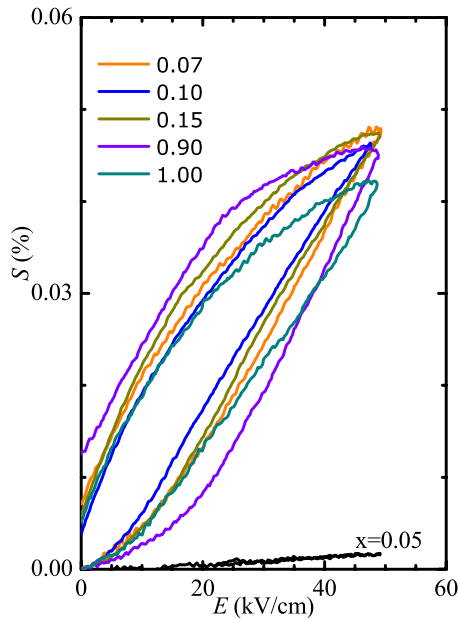


FIG. 5. (Color online) Strain obtained with a unipolar electric field at room temperature for poled ceramics samples.

$=20.5 \mu\text{C}/\text{cm}^2$ was obtained for a ceramics sample with $x = 0.10$. Such high value is nearly comparable to the P_s value of BaTiO_3 single crystal ($P_s = 26 \mu\text{C}/\text{cm}^2$).¹⁸ These results clearly show that a strong ferroelectricity is indeed realized in AKN through a chemical modification of AgNbO_3 structure with K substitution. For a K-rich region $x > x_{c3}$, normal D - E loops were also obtained. Due to the polycrystal nature of ceramics sample, we cannot make a conclusion on the exact composition dependence of P_s , which remains to be clarified in the future works on single crystals.

Along with the change in FE state with K substitution, the piezoelectricity of AKN also shows a corresponding variation. This can be seen from the S - E hysteresis loop given in the right panels of Fig. 4. Again, when $x < x_{c1}$ in which AKN has a weak ferroelectricity, we only observed an extremely low level of strain ($\sim 10^{-5}$ at $E = 50 \text{ kV}/\text{cm}$) because of the weak coupling between an electric field and a small spontaneous polarization. In contrast, when $x_{c1} \leq x \leq x_{c2}$ or $x > x_{c3}$ where the structure of AKN is transformed into a FE state with a large spontaneous polarization, a very high level of electric-field-induced strain ($\sim 8 \times 10^{-4}$ at $E = 50 \text{ kV}/\text{cm}$) was obtained.

The rather high level of strain and high Curie point of AKN with $x_{c1} \leq x \leq x_{c2}$ or $x > x_{c3}$ may be interesting for the development of lead-free piezoelectric materials. Essentially, the butterfly S - E loops shown in Fig. 4 resulted from a superimposition of the linear piezoelectric effects into the domain reorientation effects. For engineering application, the strain response under a unipolar electric field or the piezoelectric coefficient d_{33} at zero field are more important. We then performed these measurements by using poled ceramics samples. The results are summarized in Fig. 5 and Table I. A strain level of $\sim 0.05\%$ was observed for ceramics samples with $x_{c1} \leq x \leq x_{c2}$ or $x > x_{c3}$ at a unipolar electric field of 50 kV/cm. Similarly, a rather large value of d_{33} ($=46$ – $64 \text{ pC}/\text{N}$) was obtained for these samples. Through opti-

TABLE I. Strains measured with a unipolar electric field of 50 kV/cm and d_{33} values for poled AKN ceramics. The P_r values obtained from the D - E loops are also given.

x (mole)	0.05	0.07	0.10	0.90	1.00
Strain (10^{-4})	0.16	4.8	4.5	4.5	4.2
d_{33} (pC/N)	1.8	46	55	64	27
P_r ($\mu\text{C}/\text{cm}^2$)	0.14	12.0	20.5	9.6	19.0

mizing the preparation process, it may be possible to improve the piezoelectric performance of the AKN solid solution, which remains to be resolved in future works.

D. A proposed phase diagram and its relationship with the structural changes

On the basis of the results obtained from x-ray diffraction, dielectric, and FE measurements, a phase diagram is then proposed in Fig. 6(a), in which PE, FE, and AFE represent the paraelectric, ferroelectric, and antiferroelectric phases, respectively. In the figure, symmetries are also indicated on the basis of previous studies on the end numbers AgNbO_3 and KNbO_3 . To identify the symmetry of high-temperature phase of $x_{c1} < x < x_{c2}$, high-temperature structure analysis is necessary in the future works.

In order to understand this phase diagram, the changes in structural parameters including lattice constants, perovskite cell volume, and orthorhombic distortion angle β with composition are given in Figs. 6(b)–6(d). Initially, incorporating of K into the lattice of AgNbO_3 gradually reduces the PE-AFE phase transition. At the phase boundary $x = x_{c1}$, such PE-AFE transition changes to PE-FE transition. Associating with this change, lattice parameters at room temperature also change suddenly due to the transformation from the AgNbO_3 -type orthorhombic structure with weak ferroelectricity into a new orthorhombic structure with strong ferroelectricity. We can see the disappearance of the fourfold simple perovskite cell of the c -axis in the AgNbO_3 -type orthorhombic structure¹⁰ when $x > x_{c1}$. This can be attributed to the elimination of the oxygen octahedra tilting in the perovskite structure when incorporating rather larger K into the Ag site. As shown in Fig. 6(c), the substitution of K with a larger ionic radius leads to a linear increase in volume of the perovskite cell. It can be inferred that the elimination of such oxygen octahedra tilting effectively unlocks the A-site-driven strong ferroelectricity of AgNbO_3 itself in the composition range of $x_{c1} < x < x_{c2}$.³

This ferroelectricity driven mainly by the A-site atom displacement may give a reasonable explanation for the stable orthorhombic phase in these solid solutions. A well-known fact is that, in a B-site-driven FE such as BaTiO_3 and KNbO_3 , the structure is stable when B-site atom shifts off centering along the local rhombohedral direction of BO_6 octahedron at the ground state, because the available space for atom displacement along this direction is the largest. In contrast, in an A-site-driven FE, the ground state may not be a rhombohedral phase; for example, in PbTiO_3 , the FE tetragonal phase is stable down to absolute 0 K.

On the other hand, when increasing the amount of K into $x > x_{c3}$, the FE ordering in AKN changes to a B-site-driven

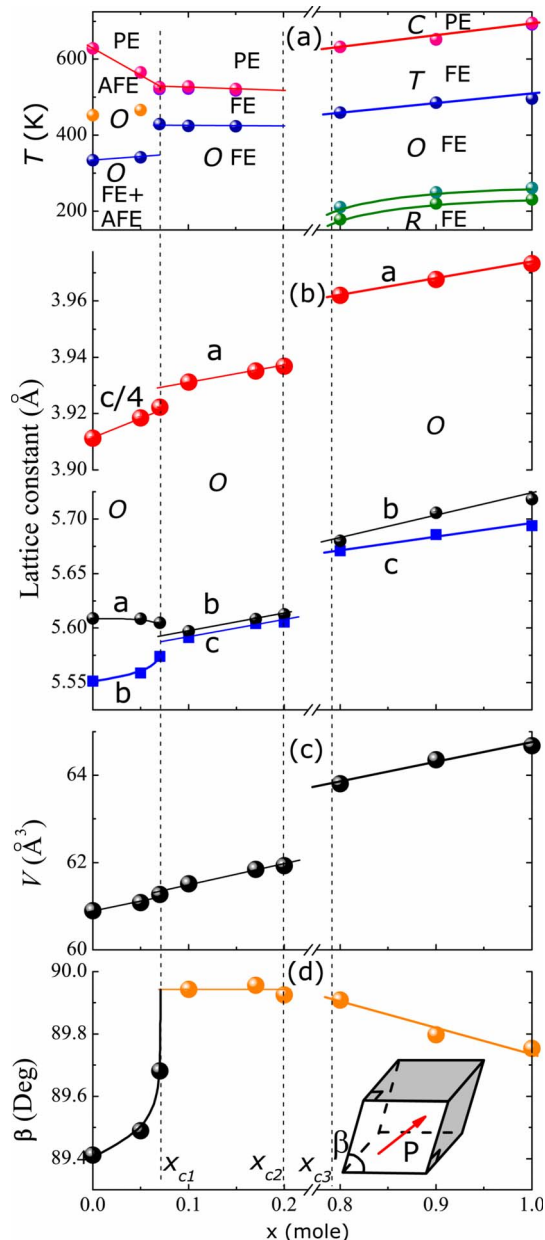


FIG. 6. (Color online) (a) A phase diagram proposed for $\text{Ag}_{1-x}\text{K}_x\text{NbO}_3$ solid solution. Phase boundaries are indicated by the lines. C, T, O, and R indicate the cubic, tetragonal, orthorhombic, and rhombohedral symmetries, respectively. PE, AFE, and FE represent paraelectric, ferroelectric, and antiferroelectric phases, respectively. (b) Lattice constants vs x . (c) Cell volume of a simple perovskite structure. (d) Orthorhombic distortion angle (β). The inset shows the orthorhombic distortion due to FE displacements along the $\langle 110 \rangle_c$ direction of the pseudocubic structure. Noted that the large orthorhombic distortion for $x < x_{c1}$ is due to the tilting of oxygen octahedrons, but not due to the FE distortion (Ref. 10).

mechanism. This can be evidenced from the facts that AKN adopts the same structure of pure KNbO_3 and shows the same sequence of FE phase transitions in the K-rich region ($x > x_{c3}$). Because KNbO_3 is a FE with a B-site-driven mechanism, the ferroelectricity in this region is then considered to be derived mainly from the Nb displacement in the oxygen octahedron. For this case, suppression of perovskite cell will reduce the available space for Nb atom displacement within the oxygen octahedron, leading to the weakening of ferroelectricity such as the decrease in Curie point.

Actually, these behaviors were observed for the K-rich AKN. As shown in Fig. 6(c), the cell volume is suppressed with the increase in Ag amount in the K-rich AKN. Associating with this suppression of perovskite cell, all FE phase transition temperatures decrease simultaneously. Therefore, in the K-rich region, Ag may be considered to take a role of a chemical pressure to suppress the unit cell.

Finally, we show an interesting relationship between the Curie point and the orthorhombic distortion angle β in AKN [Fig. 6(d)]. For $x < x_{c1}$, the large orthorhombic distortion is due to the oxygen octahedral tilting and therefore has no direct relation to the ferroelectricity. However, for $x_{c1} < x < x_{c2}$ or $x > x_{c3}$ in which strong ferroelectricity was observed, the orthorhombic distortion is essentially derived from the FE displacements [see also inset of Fig. 6(d)], and hence the orthorhombic distortion angle β may be considered as a measure of the ferroelectricity. Interestingly, similar to the compositional independence of Curie point for $x_{c1} < x < x_{c2}$, the orthorhombic distortion angle β is also independent of the composition. For $x > x_{c3}$, the FE orthorhombic distortion enhances significantly with increase in x . At the same time, Curie point increases linearly with x .

IV. SUMMARY

In summary, we investigated the FE phase evolution in the $\text{AgNbO}_3\text{--KNbO}_3$ system. In the Ag-rich region, a strong FE state with a high Curie point of ~ 525 K was realized by a chemical modification of Ag site with K substitution. The Curie point is nearly independent of the composition for $x_{c1} < x < x_{c2}$. On the other hand, in the K-rich region, AKN has the structure of pure KNbO_3 and shows the same sequence of phase transitions during cooling: cubic, tetragonal, orthorhombic, and rhombohedral. The ferroelectricity and piezoelectricity of these AKN solid solutions were also examined using the ceramics samples. Further understanding of their intrinsic physical properties requires the development of single crystals.

¹E. Cross, *Nature (London)* **432**, 24 (2004).

²T. Takenaka, K. Maruyama, and K. Sakata, *Jpn. J. Appl. Phys., Part 1* **30**, 2236 (1991).

³D. Fu, M. Endo, H. Taniguchi, T. Taniyama, and M. Itoh, *Appl. Phys. Lett.* **90**, 252907 (2007).

⁴D. Fu, M. Endo, H. Taniguchi, T. Taniyama, S. Koshihara, and M. Itoh, *Appl. Phys. Lett.* **92**, 172905 (2008).

⁵D. Fu, M. Itoh, S. Koshihara, T. Kosugi, and S. Tsuneyuki, *Phys. Rev. Lett.* **100**, 227601 (2008).

⁶S. Koveshnikov, C. Adamo, V. Tokranov, M. Yakimov, R. Kambhampati, M. Warusawithana, D. G. Schlom, W. Tsai, and S. Oktyabrsky, *Appl. Phys. Lett.* **93**, 012903 (2008).

⁷T. Tazaki, D. Fu, M. Itoh, M. Daimon, and S. Koshihara, *J. Phys.: Condens. Matter* **21**, 215903 (2009).

⁸I. Grinberg and A. M. Rappe, *Appl. Phys. Lett.* **85**, 1760 (2004).

⁹I. Grinberg and A. M. Rappe, in *Fundamental Physics of Ferroelectrics*, edited by P. K. Davies and D. J. Singh (American Institute of Physics, New York, 2003), pp. 130–138.

¹⁰Ph. Sciau, A. Kania, B. Dkhil, E. Suard, and A. Ratuszna, *J. Phys.: Condens. Matter* **16**, 2795 (2004).

¹¹M. H. Francombe and B. Lewis, *Acta Crystallogr.* **11**, 175 (1958).

¹²A. Kania, K. Roleder, and M. Lukaszewski, *Ferroelectrics* **52**, 265 (1984).

¹³D. Fu, M. Endo, H. Taniguchi, T. Taniyama, S. Koshihara, and M. Itoh (unpublished).

¹⁴D. I. Bilc and D. J. Singh, *Phys. Rev. Lett.* **96**, 147602 (2006).

- ¹⁵R. D. Shannon, *Acta Crystallogr. A* **32**, 751 (1976).
- ¹⁶B. Jaffe, W. R. Cook, Jr., and H. Jaffe, *Piezoelectric Ceramics* (Academic, London, 1971).
- ¹⁷M. E. Lines and A. M. Glass, *Principle and Application of Ferroelectrics and Related materials* (Clarendon, Oxford, 1977).
- ¹⁸*Ferroelectrics and Related Substances*, Landolt-Bornstein, New Series, Group III, Vol. 36, Pt. A1, edited by Y. Shiozaki, E. Nakamura, and T. Mitsui, (Springer, Berlin, 2001).
- ¹⁹L. Łukaszewski, *Ferroelectr., Lett. Sect.* **44**, 319 (1983).
- ²⁰D. F. Weirauch and V. Tennery, *J. Am. Ceram. Soc.* **50**, 671 (1967).
- ²¹A. Kania, *J. Phys. D* **34**, 1447 (2001).
- ²²M. Pisarski and D. Dmytrow, *Ferroelectrics* **74**, 87 (1987).